Rashba coupling in quantum dots: An exact solution

E. Tsitsishvili,[1,2] G. S. Lozano,[3,4] and A. O. Gogolin[3]
[1]*Institut für Theorie der Kondensierten Materie, Universität Karlsruhe, D-76128 Karlsruhe, Germany*
[2]*Institute for Cybernetics, Academy of Science, S. Euli 5, 380086, Tbilisi, Georgian Republic*
[3]*Department of Mathematics, Imperial College London, London SW7 2BZ, United Kingdom*
[4]*Departamento de Física, FCEyN, Universidad de Buenos Aires, cc 1428, Buenos Aires, Argentina*
(Received 17 February 2004; revised manuscript received 7 May 2004; published 22 September 2004)

We present an analytic solution to one-particle Schrödinger equation for an electron in a quantum dot with hard-wall confining potential in the presence of both magnetic field and spin-orbit coupling. Wave-functions, energy levels, and spin-flip relaxation times are calculated to all orders in the spin-orbit coupling and the magnetic field. Without the orbital contribution of the magnetic field, we find that the effective gyromagnetic ratio is strongly suppressed by the spin-orbit coupling. The spin-flip relaxation rate then has a maximum as a function of the spin-orbit coupling and is therefore suppressed in both the weak- and strong-coupling limits. In the presence of the orbital contribution of the magnetic field the effective gyromagnetic ratio changes sign in some cases.

DOI: 10.1103/PhysRevB.70.115316 PACS number(s): 71.70.Ej, 72.25.Rb, 73.21.La

I. INTRODUCTION

In recent years there has been an explosive development of research in spin physics in semiconductors. Most of it is focused on spin-related optical and transport properties of low-dimensional semiconductor structures. In particular, the spin-orbit (SO) interaction has attracted a lot of interest as it enables optical spin orientation and detection.[1] The SO coupling is (in most cases) responsible for spin relaxation. Besides, it makes the transport and spin phenomena interdependent.

SO interactions can arise in quantum dots (QDs) by various mechanisms related to electron confinement and symmetry breaking and are generally introduced in the Hamiltonian via the Rashba[2] and Dresselhaus terms.[3] The strength of these interactions not only depends on the characteristics of the material but can be controlled by an external electric field.

For most experimental realizations, quantum dots can be described as effectively two-dimensional systems in a confining potential that is usually modelled as hard-wall or harmonic confinement. In the absence of SO interactions, the effect of confinement is easily accounted for by the use of the well-known Fock-Darwin basis (harmonic potential[4]) or by an extension of the Landau problem eigenfunctions[5] to the disk geometry (hard-wall).[6]

Most of the existing theoretical studies of the spin-orbit effects in QDs rely on various perturbative schemes or numerical simulations.[7,8] For zero-magnetic field case and a hard-wall confining potential the exact analytical results have been obtained by Boulgakov and Sadreev.[9] Following the general theoretical framework of Ref. 9, we shall show in this paper that in the case of a hard-wall confinement the problem of combined spatial confinement, external magnetic field, and the SO interaction also admits an exact analytic solution. Our solution contains, as limiting cases, the Bychkov-Rashba solution (no spatial confinement),[2,10] the Bulgakov-Sadreev solutions (no external magnetic field),[9] and the Geerinckx *et al.* solution (no SO effects).[6]

The outline of the paper is as follows. We define the problem in Sec. II. In Sec. III we present an analytic solution to the problem neglecting the orbital contribution of the magnetic field (orbital effects), valid for relatively small dots. We use this solution to calculate the spin-flip relaxation rate. Next, in Sec. IV, we generalize our solution so as to include the magnetic field effects on the orbital motion of the electron. A short summary of our results is offered in Sec. V. Some more mathematical results, on the comparison of the exact solution with perturbative series and on the properties of wave functions in the presence of the orbital field, are relegated to Appendixes A and B.

II. STATEMENT OF THE PROBLEM

We consider a quasi-two-dimensional quantum dot normal to the z axis. The one-particle Hamiltonian describing an electron in such a dot is of the form

$$H = \frac{\mathbf{p}^2}{2m} + V(x,y) + \alpha_R(p_x\sigma_y - p_y\sigma_x) + \tfrac{1}{2}g\mu_B B\sigma_z, \qquad (1)$$

where m is the effective electron mass, g is the gyromagnetic ratio, μ_B is the Bohr magneton, α_R is the strength of the spin-orbit coupling, and $V(x,y)$ is the confining potential. A constant magnetic field B (parallel to the z axis) is introduced via the Zeeman term above and the Peierls substitution, $\mathbf{p}=-i\nabla-(e/c)\mathbf{A}$. The Pauli matrices are defined as standard[5] and we set $\hbar=1$. Below we use the axial gauge, $x=\rho\cos\varphi$, $y=\rho\sin\varphi$, $A_\rho=0$, and $A_\varphi=B\rho/2$. The confining potential is assumed to be symmetric, $V(x,y)=V(\rho)$. In this paper we mainly consider a hard-wall confining potential, i.e., $V(\rho)=0$ for $\rho<R$ and $V(\rho)=\infty$ for $\rho>R$, R being the radius of the dot, which is neccessary to obtain the exact solution [but we present some perturbative results for general $V(\rho)$].

We have chosen to include the Rashba term rather than the Dresselhaus term, which would be of the form

$\alpha_D(p_x\sigma_x - p_y\sigma_y)$. The two terms transform into each other under the spin rotation: $\sigma_x \leftrightarrow \sigma_y$, $\sigma_z \leftrightarrow -\sigma_z$. So our results will only need a trivial modification in the case when a solo Dresselhaus term is present. The Rashba interaction usually dominates in quantum dots obtained in a heterostructure.[7,8,11,12] There are situations when both the Rashba and the Dresselhaus terms can be included[13] but those are outside the scope of this work. Typical values of the parameters characterizing various quantum dot materials are listed in Table I. Besides, values of the g factor reported for InGaAs QDs[19] and InAs QDs[20] are also given, since they differ strongly from the bulk values.

Hamiltonian (1) rewritten in cylindrical coordinates is of the form

$$H = \begin{bmatrix} h(B) + \frac{1}{2}g\mu_B B, & \alpha_R e^{-i\varphi}\left(-\frac{d}{d\rho} + \frac{i}{\rho}\frac{d}{d\varphi} + \frac{eB}{2c}\rho\right) \\ \alpha_R e^{i\varphi}\left(\frac{d}{d\rho} + \frac{i}{\rho}\frac{d}{d\varphi} + \frac{eB}{2c}\rho\right), & h(B) - \frac{1}{2}g\mu_B B \end{bmatrix}, \tag{2}$$

where the diagonal term

$$h(B) = -\frac{1}{2m}\left[\frac{1}{\rho}\frac{d}{d\rho}\left(\rho\frac{d}{d\rho}\right) + \frac{1}{\rho^2}\frac{d^2}{d\varphi^2}\right] - \frac{i}{2}\omega_c\frac{d}{d\varphi} + \frac{1}{8}m\omega_c^2\rho^2, \tag{3}$$

and ω_c is the cyclotron frequency.

Hamiltonian (1) and (2) commutes with the z projection of the total momentum operator,

$$j_z = l_z + \tfrac{1}{2}\sigma_z, \quad l_z = -i\partial_\varphi$$

(assuming the axial gauge). The operator j_z is therefore conserved. The physical reason is that both the Rashba interaction and the magnetic field normal to the disk preserve the axial symmetry. The eigenfunctions of the total momentum operator, with a half-integer eigenvalue j, are of the following form:

$$\psi_j(\rho,\varphi) = \begin{bmatrix} e^{i(j-1/2)\varphi}f_j(\rho) \\ e^{i(j+1/2)\varphi}g_j(\rho) \end{bmatrix}. \tag{4}$$

Note that, despite the presence of the spin-orbit coupling, the variables separate in the cylindrical coordinates. This is due to the conservation of the momentum j_z. If we had included the Dresselhaus term instead of the Rashba coupling, then the operator $l_z - \frac{1}{2}\sigma_z$ would have been conserved and the variables would still separate. In zero field there is an additional symmetry $j_z \to -j_z$ related to time inversion. The states with the projections of momenta equal to j and $-j$ are Kramers doublets.[5] When the spin-orbit coupling is also switched off then the operators l_z and $\frac{1}{2}\sigma_z$ are conserved separately (with eigenvalues l and $\sigma = \pm 1/2$, $j = l + \sigma$).

The spinor components in (4) satisfy the following system of second-order ordinary differential equations:

$$\Delta^{(B)}_{j-1/2}f_j + 2m\left[E - \tfrac{1}{2}g\mu_B B - V(\rho)\right]f_j - 2m\alpha_R\nabla^B_{-,j+1/2}g_j = 0,$$

$$\Delta^{(B)}_{j+1/2}g_j + 2m\left[E + \tfrac{1}{2}g\mu_B B - V(\rho)\right]g_j - 2m\alpha_R\nabla^B_{+,j-1/2}f_j = 0, \tag{5}$$

where the spin-orbit operators are

$$\nabla^{(B)}_{\pm,j} = \pm\frac{d}{d\rho} - \frac{j}{\rho} + \frac{eB}{2c}\rho,$$

and the operator

$$\Delta^{(B)}_j = \frac{1}{\rho}\frac{d}{d\rho}\left(\rho\frac{d}{d\rho}\right) - \frac{1}{\rho^2}\left(j - \frac{eB}{2c}\rho^2\right)^2$$

is the two-dimensional Laplace operator projected onto the state with a given momentum j in the presence of the magnetic field in the axial gauge. In our convention the electron charge is $e = -|e|$, so that the cyclotron frequency is defined as $\omega_c = -eB/mc$ and the magnetic length is $a_B = \sqrt{c/|e|B}$.

TABLE I. QD parameters. (Bulk material constants of m/m_e and g are taken from Ref. 14, the Rashba parameters are taken from Refs. 15–18 and reported values of g for QDs are adopted from Refs. 19 and 20.)

QD Material	α_R(meV nm)	m/m_e	g
GaAs	2[a]	0.067	−0.44
InGaAs	10[b]–63[c]	0.041	−4.5, −0.8[e](QD)
InAs	9[b]	0.0231	−15, 1[f](QD)
InSb	25[d]	0.0139	−50.6

[a]Ref. 15 [d]Ref. 18
[b]Ref. 16 [e]Ref. 19
[c]Ref. 17 [f]Ref. 20

III. SPIN-ORBIT COUPLING AND THE ZEEMAN TERM

In this section we shall neglect the orbital contribution of the magnetic field. We leave for next section the discussion of the magnetic field effects on the orbital motion of the electron (orbital effects). Hence, $\mathbf{p} = -i\nabla$ and we keep in Hamiltonian (1) and (2) only the Zeeman term, so that the

off-diagonal elements in Hamiltonian (2) contain no B-dependent terms.

It will be convenient to work with the dimensionless coordinate $x=\rho/R$. The system of equations (5) now becomes

$$(\Delta^{(0)}_{j-1/2}+\epsilon-h)f_j-\beta_R\nabla^{(0)}_{-,j+1/2}g_j=0,$$

$$(\Delta^{(0)}_{j+1/2}+\epsilon+h)g_j-\beta_R\nabla^{(0)}_{+,j-1/2}f_j=0, \tag{6}$$

supplemented by the boundary conditions $f_j(1)=g_j(1)=0$. We have introduced two dimensionless parameters,

$$\beta_R=2\alpha_R mR, \quad h=mg\mu_B R^2 B \tag{7}$$

characterizing the strength of the spin-orbit coupling and the Zeeman term, respectively. The energy parameter is $\epsilon=2mER^2$.

(a) *Bulk solution*: In the absence of the Rashba term and confinement potential (i.e., in the bulk), the solutions regular at the origin are simply $f_j(x)\sim J_{j-1/2}(kx)$ and $g_j(x)\sim J_{j+1/2}(kx)$ with $k^2=\epsilon\pm h$, where $J_l(x)$ are the Bessel functions. The Rashba term in (6) simply acts as rising or lowering operator on the Bessel function's basis[2] since the following standard recurrence relations hold:

$$\left(\frac{d}{dx}+\frac{j+1/2}{x}\right)J_{j+1/2}(kx)=kJ_{j-1/2}(kx),$$

$$\left(\frac{d}{dx}-\frac{j-1/2}{x}\right)J_{j-1/2}(kx)=-kJ_{l+1/2}(kx).$$

This is a crucial property which allows to obtain an exact analytical solution. Indeed, the following ansatz:

$$\begin{bmatrix} f_j(x) \\ g_j(x) \end{bmatrix}=\begin{bmatrix} d_1 J_{j-1/2}(kx) \\ d_2 J_{j+1/2}(kx) \end{bmatrix} \tag{8}$$

solves the bulk problem in the presence of the spin-orbit coupling, provided that the coefficients $d_{1,2}$ satisfy the eigenvalue equation:

$$\begin{bmatrix} k^2-\epsilon+h & -\beta_R k \\ -\beta_R k & k^2-\epsilon-h \end{bmatrix}\begin{bmatrix} d_1 \\ d_2 \end{bmatrix}=0. \tag{9}$$

(b) *Disk solution*: When considering the electron confined to the disk, it is seemingly impossible to impose the vanishing boundary conditions on the ansatz (8) as Bessel functions with different indices are involved. Note, however, that as long as either β_R or h is nonzero, the bulk spectrum has two branches:

$$\epsilon=k^2\pm\sqrt{\beta_R^2k^2+h^2}.$$

Therefore for a given value of ϵ there are, in fact, two nontrivial solutions for the momentum k,

$$k_\pm^2=\frac{(2\epsilon+\beta_R^2)\pm\sqrt{\beta_R^4+4\epsilon\beta_R^2+4h^2}}{2},$$

where k_+ corresponds to a spin-down state ($\sigma=-1/2$) and k_- corresponds to a spin-up state ($\sigma=1/2$) in the $\beta_R\to 0$ limit. In order to trace the evolution of states with increasing β_R, we choose the amplitude ratios as $d_1^+/d_2^+=\alpha_+$ and $d_2^-/d_1^-=\alpha_-$, where

$$\alpha_\pm(\epsilon,\beta_R,h)=\frac{\beta_R k_\pm}{k_\pm^2-\epsilon\pm h}.$$

We are now able to satisfy the boundary conditions by combining these two linearly independent degenerate solutions,

$$\begin{bmatrix} f_j(x) \\ g_j(x) \end{bmatrix}=d^+\begin{bmatrix} \alpha_+ J_{j-1/2}(k_+x) \\ J_{j+1/2}(k_+x) \end{bmatrix}+d^-\begin{bmatrix} J_{j-1/2}(k_-x) \\ \alpha_- J_{j+1/2}(k_-x) \end{bmatrix}.$$

Indeed, the requirement that $f_j(1)=g_j(1)=0$ leads to another eigenvalue equation

$$\begin{bmatrix} \alpha_+ J_{j-1/2}(k_+) & J_{j-1/2}(k_-) \\ J_{j+1/2}(k_+) & \alpha_- J_{j+1/2}(k_-) \end{bmatrix}\begin{bmatrix} d^+ \\ d^- \end{bmatrix}=0.$$

This equation fixes the allowed energy eigenvalues as solutions to the determinant equation

$$F(\epsilon,\beta_R,h)J_{j-1/2}(k_+)J_{j+1/2}(k_-)+J_{j-1/2}(k_-)J_{j+1/2}(k_+)=0, \tag{10}$$

where the function F is defined by

$$F(\epsilon,\beta_R,h)=-\frac{\beta_R^2k_+k_-}{(k_+^2-\epsilon+h)(k_-^2-\epsilon-h)}.$$

We wish to remark that in the energy region $-h<\epsilon<h$, the momentum k_- becomes purely imaginary. One should then replace $k_-\to i\kappa_-$, κ_- being a real number. The respective Bessel function becomes a modified one, $I(\kappa_- x)$. We have found numerically that such solutions do indeed exist. These are interesting states which cannot be reached with a perturbative expansion in β_R.

For completeness we first discuss the zero-field limit already considered in Ref. 9. Indeed, in the absence of the Zeeman term we have $k_\pm=\sqrt{\epsilon+\beta_R^2/4}\pm\beta_R/2$ and $d_1^\pm=\pm d_2^\pm$ (i.e., $F=1$), so that Eq. (10) simplifies to

$$J_{j-1/2}(k_+)J_{j+1/2}(k_-)+J_{j-1/2}(k_-)J_{j+1/2}(k_+)=0, \tag{11}$$

which is the equation obtained by Bulgakov and Sadreev.[9] This equation is invariant under the change $j\to -j$ reflecting the Kramers degeneracy. At $\beta_R=0$ all states with $l\neq 0$ are fourfold degenerate, while $l=0$ states are doubly degenerate. According to the standard analysis,[5] the spin-orbit coupling splits all the $l\neq 0$ states into two Kramers doublets with $j=l+1/2$ and $j=l-1/2$, while $l=0$ states naturally remain Kramers doublets. The specifics of the Rashba term is that, at small β_R, the spin-orbit splitting (or Rashba splitting) starts at the order β_R^2.

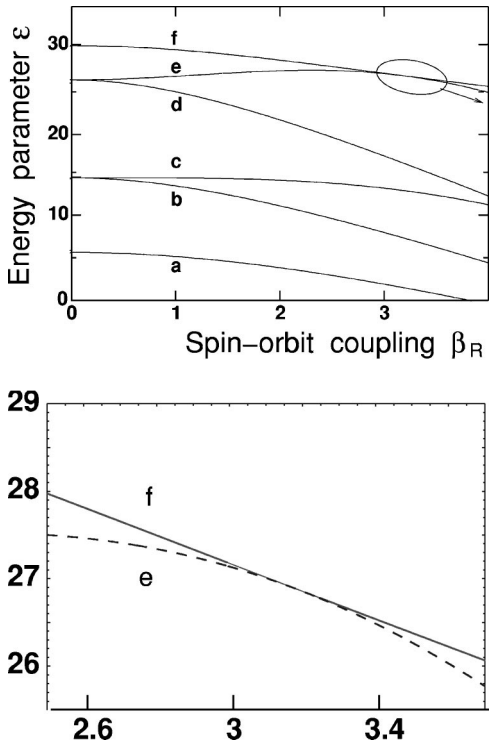

FIG. 1. Dimensionless energy ϵ as a function of β_R for the states (j,n) (n is a non-negative-integer such that $E_{j,n}<E_{j,n+1}$ at $\beta_R=0$): $(1/2,0)$ (a) (corresponds to $l=0$); $(3/2,0)$ (b) and $(1/2,1)$ (c) (correspond to $l=1$); $(5/2,0)$ (d) and $(3/2,1)$ (e) (correspond to $l=2$); and $(1/2,2)$ (f) (excited-state corresponding to $l=0$). Rashba splittings of $l\neq 0$ levels into Kramers doublets arise purely from the SO coupling in zero magnetic field ($B=0$).

We have analyzed Eq. (10) numerically, labeling the energy eigenstates as (j,n) where n is a non-negative integer such that $E_{j,n}<E_{j,n+1}$ at $\beta_R=0$. The evolution of the first few energy levels with the parameter β_R is shown in Fig. 1. (See also Ref. 9, where quite a similar evolution was found.)

In the limit $\beta_R\to 0$ the energy states shown in these figures are traced as follows: $(1/2,0)$ corresponds to $l=0$ (ground state), $(3/2,0)$ and $(1/2,1)$ correspond to $l=1$, $(5/2,0)$ and $(3/2,1)$ corresponds to $l=2$, and $(1/2,2)$ again corresponds to $l=0$ (excited state). As one can see from Fig. 1, the levels with higher j go down in energy while the levels with lower j (originating from the state with the same l at $\beta_R=0$) go up. The neighboring levels originating from the state with different l go towards each other, e.g., the levels (d) and (c) in Fig. 1. The same occurs for the levels (e) and (f) at $\beta_R<3$. For $\beta_R\sim 3$, these levels are very close and they diverge for larger β_R manifesting an avoided crossing, see the right-hand side in Fig. 1.

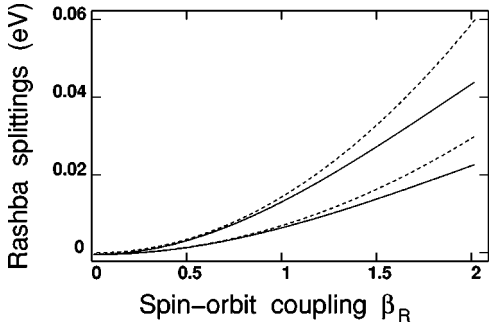

FIG. 2. Rashba splittings of $l=1$ and $l=2$ levels: energy differences $E(1/2,1)-E(3/2,0)$ and $E(3/2,1)-E(5/2,0)$ as a function of β_R. Dashed lines correspond to the same quantities calculated at the second order of perturbation theory. ($R=10$ nm, $B=0$.)

As a useful consistency check, we have verified that the β_R^2 contribution to the energy levels calculated from the exact solution coincides with that obtained via the standard perturbation theory:

$$\epsilon_{j=l+1/2,n}=\epsilon_{l,n}^{(0)}-\tfrac{1}{2}(l+1)\beta_R^2,\quad \epsilon_{j=l-1/2,n}=\epsilon_{l,n}^{(0)}+\tfrac{1}{2}(l-1)\beta_R^2, \tag{12}$$

where $\epsilon_{l,n}^{(0)}$ are the energy levels at $\beta_R=0$, that is $\epsilon_{l,n}^{(0)}=k_{l,n}^2$, $J_l(k_{l,n})=0$ and the index $n=1,2,\ldots$ numbers the zeros of the l's function in the increasing order. (We leave the details of the calculation for Appendix A.) A comparison of the exact splittings to the perturbative results (12) is shown in Fig. 2. As one can see from this figure, the first-order (in β_R^2) perturbation theory seriously overestimates Rashba splittings (by 20–30%) for $\beta_R\sim 2$. Note that, e.g., for the Rashba parameter $\alpha_R=60$ meV (realized in InGaAs dots, see Table I), $\beta_R=R(\mathrm{nm})/13$, so that the perturbation theory in this case is valid in small dots with $R\lesssim 13$ nm only.

Upon inclusion of the Zeeman term, all Kramers doublets are also split so that all the degeneracy is completely lifted. Because of inherently small values of the gyromagnetic ratio g in most semiconductor quantum dots (see Table I), the pure Zeeman splittings are small (10^{-1}–10^{-2} meV) in comparison to the characteristic energy separation between the levels of a few tens of meV. At $\beta_R\neq 0$ therefore all the (effective) Zeeman splittings can be still regarded as linear in the magnetic field,

$$\delta\epsilon_j(\beta_R)=2hF_j(\beta_R),$$

where the function $F_j(\beta_R)$ $[F(0)=1]$ plays the role of the effective gyromagnetic ratio, $g_{\mathrm{eff}}=gF(\beta_R)$, which nontrivially depends on the Rashba coupling. Indeed, expanding Eq. (10) in h, we find the following analytic formula for the gyromagnetic factor ($j>0$):

$$F_j(\beta_R)=\frac{\epsilon+\beta_R^2/4}{\beta_R\epsilon}\frac{4J_{j-1/2}(k_+)J_{j+1/2}(k_-)}{J'_{j-1/2}(k_+)J_{j+1/2}(k_-)+J_{j-1/2}(k_-)J'_{j+1/2}(k_+)+(k_+\leftrightarrow k_-)}, \tag{13}$$

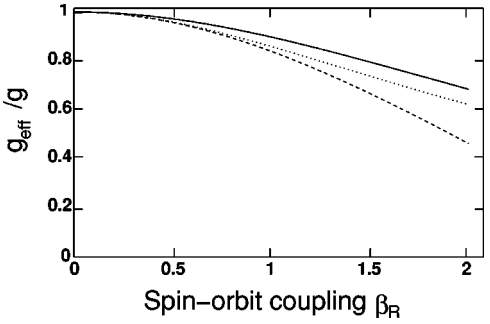

FIG. 3. Effective gyromagnetic factor as a function of β_R for the states $(1/2,0)$ (full line), $(3/2,0)$ (dotted line), $(1/2,1)$ (dashed line). ($R=10$ nm, $B=1T$.)

where ϵ and $k_\pm$ are solutions to Eq. (11). It is not difficult to expand the above function in β_R. So, for such states that $j>0$ corresponds to $\sigma=1/2$ (which include the ground state), the result is

$$F_{l+1/2}(\beta_R) = 1 - \frac{\epsilon_{l,n}^{(0)} + 2l^2 - 2}{6\epsilon_{l,n}^{(0)}}\beta_R^2. \tag{14}$$

In particular, for the ground state $l=0$,

$$F_{\frac{1}{2}}(\beta_R) = 1 - A\beta_R^2, \quad A = \frac{\epsilon_{0,0}^{(0)} - 2}{6\epsilon_{0,0}^{(0)}} \simeq 0.11. \tag{15}$$

The universal function $F_{\frac{1}{2}}(\beta_R)$ decreases monotonically (all F_j's do) from $F_{\frac{1}{2}}(0)=1$ vanishing at large β_R. Note that $F_{\frac{1}{2}}=1/2$ when $\beta_R \simeq 2.3$. The functions $F_j(\beta_R)$ are plotted in Fig. 3 for the first few levels. The fact that increasing β_R suppresses the Zeeman splitting is hardly surprising. The physical explanation is as follows. The SO coupling entangles the spin degree of freedom with the orbital one making it more difficult to polarize the Kramers doublets, which become completely rigid at large values of β_R.

As a useful consistency check, we observe that the Zeeman splittings can alternatively be calculated in perturbation theory in h (first-order correction). We then obtain

$$\delta\epsilon_j(\beta_R) = 2h\left(1 - 4\pi\int_0^1 x\, dx |g_j(x)|^2\right), \tag{16}$$

where $g_j(x)$ are zero-field wave functions. Formula (16) constitutes an alternative definition of the function $F_j(\beta_R)$ and so it must be equivalent to Eq. (13). For general β_R this equivalence translates into a rather complicated statement about intergals of Bessel function; we prove it, to the order of β_R^2, in Appendix A.

When the magnetic field is applied parallel to the dot plane, j_z is not covserved and there is (to our knowledge) no exact solution. Perturbation theory in the field still works and after an elementary calculation leads to the following result:

$$\delta\epsilon_j(\beta_R) = h[1 + F_j(\beta_R)]. \tag{17}$$

For small β_R the SO correction to the g factor is therefore twice smaller than in the case of the perpendicular field. Notice also that for large β the effective g factor is one-half of its bare value, indicating that there is a polarizable in-plane degree of freedom even in the case of a strong SO coupling.

We now turn to an application of our method and calculate the spin-flip relaxation rate. The SO coupling is the main intrinsic mechanism for electron spin-flip transitions in QDs.[15] In previous calculations of the spin-flip rates, the spin-orbit coupling was considered as a perturbation, so that the electron spin and angular momentum were assumed to be independently conserved. In the full theory this is not the case. The spin-flip transitions in fact occur between the states j and $-j$ with opposite signs of the total momentum quantum numbers. No such transition is possible within a degenerate Kramers doublet (Van Vleck cancellation). In the external magnetic field, the states j and $-j$ are split by the Zeeman interaction. The SO coupling allows then for phonon assisted transitions between the Zeeman sublevels (of a given Kramers doublet).

In what follows, we concentrate on the most interesting case and calculate the rate of the spin-flip transition between the Zeeman sublevels of the ground state ($j=\pm 1/2$). Such transition is accompanied by emission (absorption) of a phonon. Acoustic phonons dominate these processes at low temperatures. Since the Zeeman energies are small, we consider only piezoelectric interaction between the electrons and the acoustic phonons. The coupling to the piezophonons is known to be the most effective one in polar crystals for a small energy transfer.[21] Note also that we use the conventional model of bulk phonons, since the two materials in quantum dot systems usually have similar acoustic properties.[22] For the phonon mode $\mathbf{q}\alpha$ ($\mathbf{q}$ is the phonon momentum, $\alpha=l$ for a longitudinal mode and $\alpha=t$ for a transverse mode), the deformation potential applied to the $\mathbf{q}$'s Fourier component of the electron density is given by[21]

$$U_{\mathbf{q}\alpha} = \frac{1}{\sqrt{V}}\sqrt{\frac{\hbar}{2\rho_0\omega_{\mathbf{q}\alpha}}} eA_{\mathbf{q}\alpha} e^{i\,\mathbf{q}\,\mathbf{r}},$$

$$A_{\mathbf{q}\alpha} = \zeta_i\, \zeta_k\, \beta_{ikj}\, e^j_{\mathbf{q}\alpha},$$

where $\zeta=\mathbf{q}/q$ ($q=|\mathbf{q}|$), $\mathbf{e}$ is the polarization (unit) vector, ρ_0 is the mass density, $\omega_{\mathbf{q}\alpha}=s_\alpha q$ is the phonon dispersion relation, s_l, s_t are the (longitudinal and transverse) sound velocities. For crystals of interest without an inversion center (class T_d) the piezotensor β_{ikj} has only one independent component $\beta_{ikj}=h_{14}, i\neq k\neq j$. At zero temperature, the rate for the one-phonon transition within Zeeman sublevels is given by the Fermi golden rule:

$$W_{sf} = \frac{2\pi}{\hbar}\sum_{\mathbf{q}}\sum_{\mathbf{e},\alpha} |\langle\Phi^*_{-1/2}(z,\vec{\rho})|U_{\mathbf{q}\alpha}|\Phi_{1/2}(z,\vec{\rho})\rangle|^2 \delta(\Delta E_Z - \hbar\omega_{\mathbf{q}\alpha}), \tag{18}$$

where ΔE_Z is the energy difference between the states involved. For GaAs-type structures (with typical Zeeman splittings of $10^{-1}-10^{-2}$ meV), the dipole approximation ($e^{i\mathbf{q}r} \sim 1+i\mathbf{q}r$) can be used in the calculation of the electron-phonon interaction matrix element entering Eq. (18). Indeed, because of energy conservation, the matrix element in Eq.

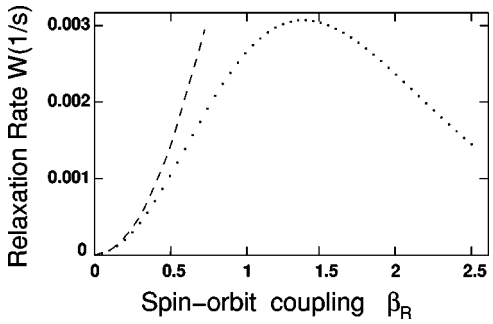

FIG. 4. The ground-state spin-flip relaxation rate W_{sf} as a function of β_R: exact calculations (dotted line), perturbative calculations (dashed line).

(18) is evaluated at the phonon momentum $q=\Delta E_Z/\hbar s$. For typical values of $s\sim 5\times 10^5$ cm/s and $\Delta E_Z \sim 10^{-1}-10^{-2}$ meV, we have $\hbar s/\Delta E_Z \sim 30-300$ nm, while R is usually about 10–20 nm (the height L_z of a quantum dot is normally much smaller than R, about 2–3 nm).

Averaging over the orientation of the **e** vector and summing over **q** then yields

$$W_{sf}=\frac{(e\ h_{14}\ R)^2\ \Delta E_Z^3}{\rho_0\hbar^4 s^5}F^2\ K, \tag{19}$$

where $s^{-5}=3/2s_l^5+1/s_t^5$, $K=8/105\pi$, and

$$F^2=\left|\int_0^{2\pi}\int_0^1 \cos\ \phi\ \psi^*_{-1/2}(x,\phi)\psi_{1/2}(x,\phi)x^2\ dx\ d\phi\right|^2. \tag{20}$$

Checking the limiting case when h and β_R are small, we obtain that the matrix element in Eq. (20) is linear over h and β_R, so that the transition rate is $W_{sf}\sim h^5\beta_R^2$, in accordance with the perturbative result of Refs. 15 and 22.

The evolution of the spin-flip transition rate given by Eq. (18) with the parameter β_R (at $B=1.5$ T) is shown in Fig. 4. (Values of $eh_{14}=1\times 10^7$ eV/cm, $s=5\times 10^5$ cm/s, and $\rho_0=5.3$ g/cm^3 are used.) Dashed line in Fig. 4 presents W_{sf} as a function of β_R calculated in the first order (in β_R^2) of the perturbation theory, while the exact calculations are presented by a dotted line. As one can see from Fig. 4, the perturbation theory overestimates the transition rates for the realistic values of the parameter β_R. An interesting new feature of the exact solution is the emergence of a maximum in the transition rate as a function of the spin-orbit coupling. The physical explanation is that while the Zeeman energy splitting decreases with β_R, the electron-phonon matrix element saturates.

Needless to say that the orbital effects of the magnetic fields may become important (for small or moderate g's) in, e.g., determining the ground-state splitting, see the next section. On the other hand, the orbital effects can be excluded by applying the magnetic field in the x-y plane. Note also that for the case of high magnetic fields (e.g., at $B\gtrsim 10$ T for GaAs structures), the dipole approximation is not valid. In this case the oscillatory behavior of the integrand in the matrix element Eq. (18) results in a suppression of the spin-flip rate.[23] An analytic calculation of the spin-flip transition rate in the presence of the orbital effects and beyond the dipole approximation is an interesting problem, which we shall address in a separate publication.[24]

IV. LANDAU-RASHBA PROBLEM IN DISK GEOMETRY

So far we have neglected the orbital contribution of the magnetic field which is not necessarily justified for many experimental setups. Fortunately, because of the very nature of the Peierls substitution, which has to be performed both in the kinetic energy term and in the spin-orbit term, the above analytic solution can be generalized to this case. In this section we proceed with such generalization.

(a) *Bulk solution*: It will be convenient to write the Schrödinger equation (5) in terms of the dimensionless variable $\xi=\rho^2/(2a_B^2)$,

$$\tilde{\Delta}_{j-\frac{1}{2}}f_j+\left(\frac{E}{\hbar w_c}-\frac{gm}{4m_e}\right)f_j-\frac{\sqrt{2}ml_b\alpha_R}{\hbar^2}\tilde{\nabla}_{-,j+\frac{1}{2}}g_j=0,$$

$$\tilde{\Delta}_{j+\frac{1}{2}}g_j+\left(\frac{E}{\hbar w_c}+\frac{gm}{4m_e}\right)g_j-\frac{\sqrt{2}ml_b\alpha_R}{\hbar^2}\tilde{\nabla}_{+,j-\frac{1}{2}}f_j=0, \tag{21}$$

where we have introduced the operators

$$\tilde{\Delta}_j=\xi\frac{d^2}{d\xi^2}+\frac{d}{d\xi}-\frac{(j+\xi)^2}{4\xi},\quad \tilde{\nabla}_{\pm,j}=\sqrt{\xi}\left(\pm\frac{d}{d\xi}-\frac{j}{2\xi}-\frac{1}{2}\right).$$

The structure of Eq. (21) suggests the following ansatz:

$$\begin{bmatrix} f_j(\xi)\\ g_j(\xi)\end{bmatrix}=\begin{bmatrix} d_1\Phi(e_0,j,\xi)\\ d_2\Phi(e_0+1,j+1,\xi)\end{bmatrix}, \tag{22}$$

where

$$\Phi(e_0,j,\xi)=\begin{cases}\left(\dfrac{\Gamma(e_0+1)}{\Gamma\left(e_0-j+\frac{1}{2}\right)}\right)^{\frac{1}{2}}\dfrac{1}{\left(j-\frac{1}{2}\right)!}\xi^{(2j-1)/4}\exp\left(-\dfrac{\xi}{2}\right)M\left(j-\dfrac{1}{2}-e_0,j+\dfrac{1}{2};\xi\right), & j>0,\\ \left(\dfrac{\Gamma\left(e_0-j+\frac{3}{2}\right)}{\Gamma(e_0+1)}\right)^{\frac{1}{2}}\dfrac{(-1)^{-j+1/2}}{\left(-j+\frac{1}{2}\right)!}\xi^{-(2j-1)/4}\exp\left(-\dfrac{\xi}{2}\right)M\left(-e_0,-j+\dfrac{3}{2};\xi\right), & j<0.\end{cases} \tag{23}$$

Here $M(a,c;\xi)$ is the confluent hypergeometric series satisfying $\xi M''+(c-\xi)M'-aM=0$ (see Ref. 25). The prefactors in (23) are inspired by those occurring in the standard Landau problem[5] but it should be noted that the eigenfunctions are *not* normalized. The energy parameter e_0 is to be determined.

Clearly (23) solves (21) without the Rashba term. The basic property which allows a simple solution is again that the operators $\tilde{\nabla}_{+,j-1/2}$ and $\tilde{\nabla}_{-,j+1/2}$, involved in the Rashba term, act as rising and lowering operators on the proposed eigenfunctions. Indeed, as shown in Appendix B,

$$\tilde{\nabla}_{+,j-1/2}\Phi(e_0,j,\xi) = -\sqrt{e_0+1}\,\Phi(e_0+1,j+1,\xi),$$

$$\tilde{\nabla}_{-,j+1/2}\Phi(e_0+1,j+1,\xi) = -\sqrt{e_0+1}\,\Phi(e_0,j,\xi). \quad (24)$$

Therefore in the basis (22) and (23), the Schrödinger equation (21) reduces to an algebraic system,

$$\begin{pmatrix} e-e_0-s & \gamma\sqrt{e_0+1} \\ \gamma\sqrt{e_0+1} & e-e_0+s-1 \end{pmatrix}\begin{pmatrix} d_1 \\ d_2 \end{pmatrix} = 0. \quad (25)$$

The determinant equation of the form

$$(e-e_0-s)(e-e_0+s-1)-\gamma^2(e_0+1)=0 \quad (26)$$

follows. We have introduced dimensionless parameters $e=E/\omega_c-1/2$ for the energy (not to be confused with the electron charge), $\gamma=\alpha_R(2m/\omega_c)^{1/2}$ for the spin-orbit coupling (note that this parameter is different from β_R previously defined), and $s=gm/(4m_e)$ for the Zeeman coupling. Here m_e is the electron mass, while m is the effective electron mass for the material in question.

Now in the bulk, a normalizable solution is obtained only when $M(a,c;\xi)$ reduces to a (Laguerre) polynomial, that is when $a=-n_\rho$, n_ρ being a non-negative integer. The energy parameter e_0 is therefore fixed as $e_0=n_\rho+j-1/2$ for $j>0$ and $e_0=n_\rho$ for $j<0$. It is easy to see that the energy spectrum is then parametrized by a single positive integer $n=e_0+1$ and the determinant equation (26) reduces to the expression

$$e=e_n=n-\tfrac{1}{2}\pm\sqrt{\left(s-\tfrac{1}{2}\right)^2+\gamma^2 n^2}, \quad (27)$$

in full agreement with the known result.[10] Note also that $s=1/2$ is the supersymmetric point of the Landau problem.

(b) *Disk solution*: Next we consider the disk geometry, i.e., the boundary condition $f_j(\xi_0)=g_j(\xi_0)=0$ $[\xi_0=R^2/(2a_B^2)]$ replaces the bulk requirement that the wave functions be normalizable. There is therefore no simple restriction on the parameter e_0. We can still proceed as in Sec. III because, for a given value of the energy e, there are two nontrivial solutions for e_0 of the determinant equation (26):

$$e_0^{\pm}=\frac{2e-1+\gamma^2\pm\sqrt{(\gamma^2+1)^2+4e\gamma^2+4(s^2-s)}}{2}.$$

Hence, in the bulk, there are two degenerate solutions of the Schrödinger equation that must be combined in the general solution

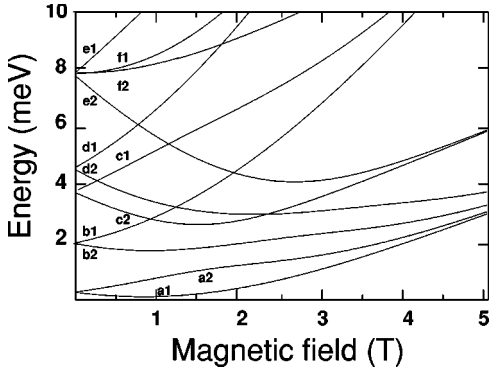

FIG. 5. The energy spectrum calculated by using Eq. (28). Energy as a function of magnetic field B for the states (degenerate at $B=0$): $(1/2,0)$ (a1) and $(-1/2,0)$ (a2), $(3/2,0)$ (b1) and $(-3/2,0)$ (b2), $(1/2,1)$ (c1) and $(-1/2,1)$ (c2), $(5/2,0)$ (d1) and $(-5/2,0)$ (d2), $(3/2,1)$ (e1) and $(-3/2,1)$ (e2), and $(1/2,2)$ (f1) and $(-1/2,2)$ (f2). ($R=50$ nm, $\beta_R=3.35$.)

$$\Psi(\xi)=\begin{pmatrix} d_1^+\Phi(e_0^+,j,\xi)+d_1^-\Phi(e_0^-,j,\xi) \\ d_2^+\Phi(e_0^++1,j+1,\xi)+d_2^-\Phi(e_0^-+1,j+1,\xi) \end{pmatrix}.$$

The ratios of the amplitudes in the above equation are fixed by Eq. (25) as

$$\frac{d_1^{\pm}}{d_2^{\pm}}=\gamma\frac{(e_0^{\pm}+1)^{\frac{1}{2}}}{e_0^{\pm}-e+s}$$

still leaving two amplitudes arbitrary. Imposing the disk boundary condition $\Psi(\xi_0)=0$ gives yet another eigenvalue equation, the determinant of which is

$$\frac{(e_0^++1)^{\frac{1}{2}}}{e_0^+-e+s}\Phi(e_0^+,l,\xi_0)\Phi(e_0^-+1,l+1,\xi_0) - \frac{(e_0^-+1)^{\frac{1}{2}}}{e_0^--e+s}\Phi(e_0^-,l,\xi_0)\Phi(e_0^++1,l+1,\xi_0)=0. \quad (28)$$

This equation is exact and provides (implicitly) all the information about the energy spectrum of the problem. We have investigated Eq. (28) numerically for some characteristic values of the parameters. For the values of $|g|=0.44$, $m=0.067m_e$, and $\beta_R=3.35$, the evolution of the first few energy levels with the magnetic field is shown in Fig. 5. The energy states shown in this figure are traced similarly as in the case of Fig. 1. The main features of the energy spectrum in the magnetic field are the following. The Kramers doublet splitting is pronounced even for the ground state $l=0$ [labeled as the level (a) in Fig. 5]. The splitting energy in this case reaches the value of ~ 0.5 meV at $B=1$ T and strongly exceeds the pure Zeeman splitting equal to $|g|\mu_B B/2 \sim 0.03$ meV (for $|g|=0.44$ and $B=1$ T). In the absence of the spin-orbit coupling, however, the only one reason to split the ground state is the Zeeman interaction. Indeed, at $\beta_R=0$ there is no orbital contribution of the magnetic field for the states with $l=0$.[5] One can see in Fig. 5 also that for the levels originating from the same $l\neq 0$ (at $\beta_R=0$), the Kramers doublets splittings are different by values, which is not the case

again at $\beta_R=0$.[5] For example, the levels labeled as (b), (b1), (b2) and (c), (c1), (c2) in this figure correspond to $l=1$, with approximately 2 times larger splitting for the latter level than for the former one (at $B=1$ T). It is therefore the combined effect of the Rashba term and the orbital contribution of the magnetic field that lifts the Kramers degeneracy and leads to the above pecularities for the energy spectrum. So, the orbital contribution can clearly not be neglected in this case.

The SO effects on the pure Zeeman splitting were investigated in the preceding section, here we consider the splittings resulting from the orbital contribution of the magnetic field. General analytic results can be obtained at the first order in the magnetic field, to which case we restrict the following calculations. Let us write down the part of the Hamiltonian linear in the magnetic field,

$$H_B=\frac{1}{2}g\mu_B B\sigma_z+\frac{1}{2}\omega_c l_z-\frac{|e|B}{2c}\alpha_R\rho(\sigma_x\cos\varphi+\sigma_y\sin\varphi). \tag{29}$$

The above perturbation results in the splitting between the j and $-j$ states, which is linear in the magnetic field. Its magnitude is simply determined by the matrix elements of H_B with respect to the zero-field wave functions (4),

$$\delta\epsilon_j(\beta_R)=2hF_j(\beta_R)+\frac{h}{2s}[1-F_j(\beta_R)]-\frac{h}{s}R_j(\beta_R)+\frac{h}{s}(j-1/2), \tag{30}$$

where $(j>0)$

$$R_j(\beta_R)=\pi\beta_R\int_0^1 x^2\,dx[f_j^*(x)g_j(x)+g_j^*(x)f_j(x)]. \tag{31}$$

Therefore the total ground-state g factor, involving both the pure Zeeman and the orbital contributions, and exact to all orders in the SO coupling, is of the form

$$g_{\rm eff}(\beta_R)=gF_{\frac{1}{2}}(\beta_R)+\frac{g}{4s}[1-F_{\frac{1}{2}}(\beta_R)]-\frac{g}{2s}R_{\frac{1}{2}}(\beta_R), \tag{32}$$

where the ratio $g/(4s)=m_e/m$ is positive while the bare g-factor g can have either sign. The first term in (32) describes the suppression of the matrix elements of σ_z by the SO coupling as discussed in the preceding section. The second term in (32) is a standard orbital contribution (vanishing at $\beta_R=0$) to the g factor and it is positive. This is because the Rashba coupling mixes the state $(l=0,\sigma=1/2)$ with the state $(l=1,\sigma=-1/2)$ and the state $(l=0,\sigma=-1/2)$ with the state $(l=-1,\sigma=1/2)$ and therefore the average momentum $\langle 1/2|l_z|1/2\rangle>0$, while $\langle -1/2|l_z|-1/2\rangle<0$. The third term in (32) is a mixed contribution to the g factor resulting from an interplay between the orbital effect and SO coupling. The mixed contribution turns out to be negative. In fact, for small β_R, the mixed contribution is exactly (-2) times the orbital contribution thus effectively changing sign of the full orbital term. This statement is true for any confining potential. Indeed, the zero-field functions f_j and g_j satisfy Eq. (5) with $B=0$. Expanding this system of equations in β_R one can show that at the first order

$$g_j(x)=\frac{\beta_R x}{2}f_j^{(0)}(x), \tag{33}$$

where $f_j^{(0)}(x)$ is the $h=\beta_R=0$ solution of the problem with arbitrary $V(\rho)$. Therefore

$$1-F_j(\beta_R)=R_j(\beta_R)=\pi\beta_R^2\int_0^1 x^3\,dx|f_j^{(0)}(x)|^2$$

to the order of β_R^2.

For the particular case of the hard-wall potential,

$$f^{(0)}_{j=l+1/2}(x)=\frac{J_l(k_{l,n}x)}{\sqrt{\pi}\,J_{l+1}(k_{l,n})},$$

$$R_{j=l+1/2}(\beta_R)=\frac{\beta_R^2}{J_{l+1}^2(k_{l,n})}\int_0^1 x^3\,dx\,J_l^2(k_{l,n}x), \tag{34}$$

where $J_l(k_{l,n})=0$. As a result, for weak SO coupling the g factor expands according to Eq. (15),

$$g_{\rm eff}(\beta_R)=g\left[1-\left(\frac{1}{4s}+1\right)A\beta_R^2\right]. \tag{35}$$

For $g<0$ (small β_R), the Zeeman and the (full) orbital contributions are both negative and so is $g_{\rm eff}(\beta_R)$. $|g_{\rm eff}(\beta_R)|$ increases or decreases with β_R depending on the material parameter s being less or greater than $1/4$. At $s\sim 1/4$, $g_{\rm eff}(\beta_R)$ is (almost) independent of β_R. In addition, when $s\ll 1$, the characteristic scale of the SO coupling, over which $g_{\rm eff}(\beta_R)$ changes fast, is $\beta_R\sim\sqrt{s/A}$. Note that the parameters used in Fig. 5 are such that s is very small, $s\sim 0.03$, and the bare g factor is negative $(g=-0.44)$. For this case therefore $|g_{\rm eff}|$ increases with β_R resulting in a large effective Zeeman splitting of the ground state $l=0$ discussed above. For $g>0$ the Zeeman and the orbital contributions compete. The orbital contribution is smaller than the Zeeman one at small β_R but always prevails with increasing β_R resulting in the change of sign of $g_{\rm eff}(\beta_R)$. The change of sign occurs at $\beta\simeq 2.5$ for $s\sim 1$ and at $\beta_R\sim\sqrt{s/A}$ for $s\ll 1$.

Note that if we include the Dresselhaus term instead of the Rashba term, then the unitary transformation

$$U=\frac{1}{\sqrt{2}}(\sigma_x+\sigma_y)$$

of Hamiltonian (1) with the Rashba term results into the Hamiltonian $UHU^\dagger$ which now involves the Dresselhaus type term $(\alpha_R\to\alpha_D)$ but the sign of the Zeeman term is reversed. Therefore, in the presence of the solo Dresselhaus term, formula (32) reads

$$g_{\rm eff}(\beta_D)=gF_{\frac{1}{2}}(\beta_D)-\frac{g}{4s}\left[1-F_{\frac{1}{2}}(\beta_D)\right]+\frac{g}{2s}R_{\frac{1}{2}}(\beta_D), \tag{36}$$

where $\beta_D=2\alpha_D mR$. As mentioned above our solution fails when both the Rashba and the Dresselhaus terms are present.

It is clear, however, that there are no processes mixing them up to and including the third order of perturbation theory in $\beta_{R,D}$, so we may write

$$g_{\rm eff}(\beta_R,\beta_D)=g\left[1-\left(\frac{1}{4s}+1\right)A\beta_R^2+\left(\frac{1}{4s}-1\right)A\beta_D^2\right]. \tag{37}$$

This perturbative formula is universal in the sense that only the dimesionless constant A depends on the shape of the confining potential. Similar dependence of the effective g factor on the Rashba and the Dresselhaus coupling strength was obtained in Ref. 23 for a parabolic confining potential.

We close this section by performing a consistency check. Let us compare the exact result Eq. (30) with the standard perturbation theory. We calculated the correction in β_R and h to the energy levels by means of the standard perturbative expansion and found

$$\epsilon_{j=\pm l-1/2,n}=\epsilon_{l,n}^{(0)}-h(1-8\beta_R^2S_{l,n})\pm\frac{lh}{2s}\pm\frac{1}{2}\beta_R^2(l\mp1)+2\beta_R^2\frac{h}{s}S_{l,n},$$

$$\epsilon_{j=\pm l+1/2,n}=\epsilon_{l,n}^{(0)}+h(1-8\beta_R^2S_{l,n})\pm\frac{lh}{2s}\mp\frac{1}{2}\beta_R^2(l\pm1)-2\beta_R^2\frac{h}{s}S_{l,n}, \tag{38}$$

where the object

$$S_{l,n}=\frac{\epsilon_{l,n}^{(0)}+2l^2-2}{48\ \epsilon_{l,n}^{(0)}},$$

is calculated in Appendix A. The resulting energy splittings coincide with those given by formula (30) when expansion (14) is used and with formula (12) at $h=0$.

V. CONCLUSIONS

We presented an analytic solution to the problem of an electron in a quantum dot in the presence of both the magnetic field and the spin-orbit coupling. The method rests on the observation that there are in this problem two degenerate eigenfunctions in the bulk that can be combined to satisfy the boundary conditions for both spinor components.

We calculated the energy levels, the real-space wave functions, and various quantities of physical interest. The Rashba energy splittings are overestimated in the first-order (in β_R^2) perturbation theory. There is a strong suppression of effective gyromagnetic ratio by the spin-orbit coupling (without the orbital contribution of the magnetic field). The spin-flip relaxation rate has a maximum as a function of the spin-orbit coupling. Inclusion of the orbital effects gives rise to quite rich magneto-optical spectra. In particular, the combined effect of the orbital contribution and the Rashba term results in a large splitting of the ground state. The effective g factor changes sign with β_R if the bare g factor is positive. We hope that our method can be used in future research for obtaining further interesting results on the spin-orbit effects in quantum dots; in particular, it would be interesting to investigate spin-flip transitions in high magnetic fields.

ACKNOWLEDGMENTS

The authors are grateful to Levitov, who has independently arrived at a similar solution with Rashba,[26] for interesting discussions and to Sadreev for calling our attention to Ref. 9. The research by G.L. and A.O.G. is supported by the EPSRC of the UK under Grants Nos. GR/N19359 and GR/R70309 and the EU training network DIENOW. The research by E.T. is supported by the Center for Functional Nanostructures (CFN) of the Deutsche Forschungsgemeinschaft (DFG) within project A2.

APPENDIX A: PERTURBATIVE EXPANSION IN β_R AND h

In this appendix we elaborate on the perturbative results for the Rashba splittings. We recall that, at $\beta_R=h=0$, the energy levels, $\epsilon_{l,n}^{(0)}=k_{l,n}^2$, are determined from the equation $J_l(k_{l,n})=0$, where the index $n=1,2,...$ numbers the zeros of the l's Bessel function in increasing order.

At $h=0$, expanding Eq. (11) up to second order in β_R leads to Eq. (12) for the perturbative corrections to the eigenstates. Notice that the second-order correction does not depend on n. Also, the levels with higher j go down in energy while the levels with lower j (originating from the state with the same l at $\beta_R=0$) go up, the Rashba splitting being $\epsilon_{j=l-1/2,n}-\epsilon_{j=l+1/2,n}=l\beta_R^2$.

On the other hand, employing the standard perturbation theory, one can easily see that the effective second-order secular equation has only diagonal matrix elements involving the standard Lommel's integrals with the Bessel functions and thus obtain[27]

$$\epsilon_{j=l\pm1/2,n}-\epsilon_{l,n}^{(0)}=4\beta_R^2\sum_{m=1}^{\infty}\frac{k_{l,n}^2k_{l\pm1,m}^2}{(k_{l,n}^2-k_{l\pm1,m}^2)^3}, \tag{A1}$$

for $h=0$. Furthermore, at the first order in h (still second order in β_R) one finds Eq. (38) for the energy corrections, where

$$S_{l,n}^{\pm}=k_{l,n}^2\sum_{m=1}^{\infty}\left[\frac{k_{l\pm1,m}^2}{(k_{l,n}^2-k_{l\pm1,m}^2)^4}\right],$$

$$\mathcal{R}_{l,n}^{\pm}=\frac{k_{l,n}}{2J_{l+1}(k_{l,n})}\sum_{m=1}^{\infty}\frac{k_{l\pm1,m}\int_0^1x^2\,dx\,J_{l\pm1}(k_{l\pm1,m}x)J_l(k_{l,n}x)}{(k_{l\pm1,m}^2-k_{l,n}^2)^2J_{l+1\pm1}(k_{l\pm1,n})}. \tag{A2}$$

It turns out (see below) that $\mathcal{S}_{l,n}^{+}=\mathcal{S}_{l,n}^{-}\equiv\mathcal{S}_{l,n}$, $\mathcal{R}_{l,n}^{+}=\mathcal{R}_{l.n}^{-}\equiv\mathcal{R}_{l,n}$, and $\mathcal{R}_{l,n}=\mathcal{S}_{l,n}$.

Thus, the technical problem here is to analytically perform the summation over zeros of the Bessel functions. This

can be achieved by using the product representation formula for the Bessel function (see, e.g., Ref. 27),

$$J_m(z) = \frac{z^m}{2^m\Gamma(m+1)}\prod_{n=1}^{\infty}\left(1-\frac{z^2}{k_{m,n}^2}\right), \tag{A3}$$

where $J_m(k_{m,n})=0$. Indeed, define

$$h_0(z_\pm,m) = \sum_n \ln\left(1-\frac{z_\pm^2}{k_{m,n}^2}\right), \quad h_p(z_\pm) = \sum_n \frac{1}{(k_{m,n}^2 - z_\pm^2)^p},$$

with $z_\pm$ satisfying $J_{m\pm1}(z_\pm)=0$ and p being a positive integer. Upon repeated differentiation in z of formula (A3) and subsequent usage of Bessel functions' recurrence relations, it is easy to see that

$$h_1(z_+,m)=0, \quad h_2(z_+,m)=\frac{z_+^2}{4}, \quad h_3(z_+,m)=-\frac{1}{4z_+^4}-\frac{m}{8z_+^4}, \quad h_4(z_+,m)=\frac{1}{4z_+^6}+\frac{5m+m^2}{24z_+^6}+\frac{1}{48z_+^4},$$

$$h_1(z_-,m)=\frac{m}{z_-^2}, \quad h_2(z_-,m)=\frac{1}{4z_-^2}-\frac{m}{z_-^4}, \quad h_3(z_-,m)=\frac{m}{z_-^6}-\frac{1}{4z_-^4}+\frac{m}{8z_-^4}, \quad h_4(z_-,m)=-\frac{m}{z_-^8}+\frac{6-5m+m^2}{24z_-^6}+\frac{1}{48z_-^4}.$$

Expressing the right-hand-sides of Eqs. (A1) and (A2) as linear combinations of h's found above, we immediately obtain

$$\sum_{n'}^{\infty}\frac{k_{l\pm1,n'}^2}{(k_{l,n}^2-k_{l\pm1,n'}^2)^3} = -\frac{\pm l+1}{8k_{l,n}^2}, \quad S_{l,n}=\frac{-2+2l^2+k_{l,n}^2}{48k_{l,n}^2},$$

which justifies the results, Eqs. (12) and (38), quoted in the main text.

Using the summation representation formula for the Bessel function (see, e.g., Ref. 28)

$$J_m(kz) = 2J_m(k)\sum_{n=1}^{\infty}\frac{k_{m,n}J_m(k_{m,n}z)}{(k_{m,n}^2-k^2)J_{m+1}(k_{m,n})}, \tag{A4}$$

where $J_m(k_{m,n})=0$, we obtain

$$\mathcal{R}_{l,n} = \frac{1}{8J_{l+1}^2(k_{l,n})}\int_0^1 x^3\,dx\,J_l^2(k_{l,n}x) \tag{A5}$$

which justify the result, Eq. (34), quoted in the main text. Performing the integration over x in Eq. (A5), for the ground state $l=0$ we obtain

$$\mathcal{R}_{0,0} = \frac{1}{8J_1^2(k_{0,0})}\int_0^1 x^3\,dx\,J_0^2(k_{0,0}x) = \frac{k_{0,0}^2-2}{48k_{0,0}^2},$$

which is in accordance with expression (15) in the main text.

Finally, note that the following representation for the Bessel function holds:

$$\mathcal{I}_l(z) = \frac{1}{J_{l+1}^2(z)}\int_0^z x^3\,dx\,J_l^2(x) = \frac{z^4+2(l^2-1)z^2}{6}, \tag{A6}$$

where $J_l(z)=0$. Straightforward calculations (by using the Lommel's integrals[28]) proof expression (A6). In particular case of $l=0,1,2,3$, e.g., one obtains

$$\mathcal{I}_0(z)=\frac{z^4-2z^2}{6}, \quad \mathcal{I}_1(z)=\frac{z^4}{6}, \quad \mathcal{I}_2(z)=\frac{z^4+6z^2}{6},$$

$$\mathcal{I}_3(z)=\frac{z^4+16z^2}{6}.$$

APPENDIX B: WAVE FUNCTIONS FOR THE LANDAU-RASHBA PROBLEM

In this appendix we supply more details of the solution of the Landau-Rashba problem. Upon the substitution

$$\begin{bmatrix} f_j \\ g_j \end{bmatrix} = e^{-\xi/2}\begin{bmatrix} \xi^{|j-1/2|/2}F_j \\ \xi^{|j+1/2|/2}G_j \end{bmatrix}, \tag{B1}$$

the Schrödinger equation becomes, explicitly

$$\left[\xi\frac{d^2}{d\xi^2}+\left(j+\frac{1}{2}-\xi\right)\frac{d}{d\xi}-j+\frac{1}{2}+e-s\right]F_j+\gamma\left[\xi\frac{d}{d\xi}+j+\frac{1}{2}\right]G_j=0,$$

$$\left[\xi\frac{d^2}{d\xi^2}+\left(j+\frac{3}{2}-\xi\right)\frac{d}{d\xi}-j-\frac{1}{2}+e+s\right]G_j-\gamma\left[\frac{d}{d\xi}-1\right]F_j=0$$

for $j>0$, and

$$\left[\xi\frac{d^2}{d\xi^2}+\left(-j+\frac{3}{2}-\xi\right)\frac{d}{d\xi}e-s\right]F_j+\gamma\frac{d}{d\xi}G_j=0,$$

$$\left[\xi\frac{d^2}{d\xi^2}+\left(-j+\frac{1}{2}-\xi\right)\frac{d}{d\xi}+e+s\right]G_j-\gamma\left[\xi\frac{d}{d\xi}-j+\frac{1}{2}-\xi\right]F_j=0$$

for $j<0$. Using standard relations satisfied by the confluent hypergeometric functions (see Ref. 25) we obtain the following identities for the basis wave function:

$$\left[\frac{d}{d\xi}-1\right]M\left(j-\frac{1}{2}-e_0,j+\frac{1}{2};\xi\right)=-\frac{e_0+1}{j+1/2}M\left(j-\frac{1}{2}-e_0,j+\frac{3}{2};\xi\right),$$

$$\left[\xi\frac{d}{d\xi}+j+\frac{1}{2}\right]M\left(j-\frac{1}{2}-e_0,j+\frac{3}{2};\xi\right)=\left(j+\frac{1}{2}\right)M\left(j-\frac{1}{2}-e_0,j+\frac{1}{2};\xi\right),$$

$$\frac{d}{d\xi}M\left(-e_0-1,-j+\frac{1}{2};\xi\right)=-\frac{e_0+1}{-j+1/2}M\left(-e_0,j+\frac{3}{2};\xi\right),$$

$$\left[\xi\frac{d}{d\xi}-j+\frac{1}{2}-\xi\right]M\left(-e_0,-j+\frac{3}{2};\xi\right)=(-j+1/2)M\left(-e_0-1,-j+\frac{1}{2};\xi\right).$$

These identities, together with the definition (23), lead to the basic property (24) that allows for the solution of the Landau-Rashba problem.

[1] G. E. Pikus and A. N. Titkov, *Optical Orientation*, edited by F. Meier and B. P. Zakharchenya (North-Holland, Amsterdam, 1984).

[2] E. I. Rashba, Fiz. Tverd. Tela (Leningrad) **2**, 1224 (1960) [Sov. Phys. Solid State **2**, 1109 (1960)].

[3] G. Dresselhaus, Phys. Rev. **100**, 580 (1955).

[4] L. Jacak, A. Wójs, and P. Hawrylak, *Quantum Dots* (Springer-Verlag, Berlin, 1998).

[5] L. D. Landau and I. M. Lifshitz, *Quantum Mechanics* (Pergamon, New York, 1965).

[6] F. Geerinckx, F. M. Peeters, and J. T. Devreese, J. Appl. Phys. **68**, 3435 (1990).

[7] M. Governale, Phys. Rev. Lett. **89**, 206802 (2002), and references therein.

[8] S. Bandyopadhyay, Phys. Rev. B **61**, 13 813 (2000).

[9] E. N. Bulgakov and A. F. Sadreev, JETP Lett. **73**, 505 (2001).

[10] Yu. A. Bychkov and E. I. Rashba, Pis'ma Zh. Eksp. Teor. Fiz. **39**, 66 (1984) [JETP Lett. **39**, 78 (1984)]; J. Phys. C **17**, 6039 (1984).

[11] The spin-orbit interaction due to the parabolic (lateral) confining potential in the dot has been discussed in Ref. 12. For a hard-wall potential additional SO terms have no effect due to the vanishing boundary conditions.

[12] O Voskoboynikov, C. P. Lee, and O. Tretyak, Phys. Rev. B **63**, 165306 (2001).

[13] J. Schliemann, J. C. Egues, and D. Loss, Phys. Rev. Lett. **90**, 146801 (2003).

[14] Landolt-Börnstein, New Series, edited by O. Madelung, M. Schultz, and H. Weiss (Springer-Verlag, Berlin, 1982), Vol. 17a,b, Group III, Vol. 22a, Group III.

[15] A. V. Khaetskii and Yu. V. Nazarov, Phys. Rev. B **61**, 12 639 (2000); **64**, 125316 (2001).

[16] J. Nitta, T. Akazaki, H. Takayanagi, and T. Enoki, Phys. Rev. Lett. **78**, 1335 (1997); G. Engels, J. Lange, T. Schapers, and H. Luth, Phys. Rev. B **55**, R1958 (1997).

[17] L. J. Cui, Y. P. Zeng, B. Q. Wang, Z. P. Zhu, L. Y. Lin, C. P. Jiang, S. L. Guo, and J. H. Chu, Appl. Phys. Lett. **80**, 3132 (2002).

[18] C. F. Destefani, S. E. Ulloa, and G. E. Marques, Phys. Rev. B **69**, 125302 (2004).

[19] M. Bayer, A. Kuther, A. Forchel, A. Gorbunov, V. B. Timofeev, F. Schäfer, J. P. Reithmaier, T. L. Reinecke, and S. N. Walck, Phys. Rev. Lett. **82**, 1748 (1999).

[20] A. S. G. Thornton, T. Ihn, P. C. Main, L. Eaves, and M. Henini, Appl. Phys. Lett. **73**, 354 (1998);G. Medeiros-Ribeiro, M. V. B. Pinheiro, and V. L. Pimentel, and E. Magera, *ibid.* **80**, 4229 (2002).

[21] V. F. Gantmakher and Y. B. Levinson, *Carrier Scattering in Metals and Semiconductors* (North-Holland, Amsterdam, 1987).

[22] L. M. Woods, T. L. Reinecke, and Y. Lynda-Geller, Phys. Rev. B **66**, 161318(R) (2002).

[23] R. de Sousa and S. Das Sarma, Phys. Rev. B **68**, 155330 (2003).

[24] E. Tsitsishvili, G. S. Lozano, and A. O. Gogolin (unpublished).

[25] Bateman Manuscript Project, *Higher Transcendental Functions* (Bateman, New York, 1953).

[26] L. Levitov and E. I. Rashba (private communication).

[27] G. N. Watson, *A Tretise on the Theory of the Bessel Functions* (Cambridge University Press, Cambridge, 1992).

[28] F. Bowman, *Introduction to Bessel Functions* (Dover, New York, 1958).